

## Multi-Method Observations and Modelling of the Three-Dimensional Currents Associated with a Very Strong Ps6 Event

G. Gustafsson<sup>1</sup>, W. Baumjohann<sup>2</sup>, and I. Iversen<sup>3</sup>

<sup>1</sup> Kiruna Geophysical Institute, S-981 27 Kiruna, Sweden

<sup>2</sup> Institut für Geophysik der Universität Münster, Gievenbecker Weg 61, D-4400 Münster, Federal Republic of Germany

<sup>3</sup> Danish Space Research Institute, DK-2800 Lyngby, Denmark

**Abstract.** A pulsation event has been studied which showed Ps6-type characteristics with a period of about 20 min. Data from a number of magnetometer and riometer measurements over a large area have been combined with balloon measurements of the electric field to obtain a detailed description of the ionospheric current system during the event. The pulsations reported here occurred over an interval longer than 3 h and showed large magnetic variations, up to 700 nT. A model of the three-dimensional current flow has been derived which agrees with the data. It is concluded that most of the magnetic disturbance measured on the ground is caused by Hall-currents.

**Key words:** Auroral zone – Magnetic fields – Electric fields – Riometer absorption – Ps6 pulsations – Omega bands – Three-dimensional current systems

### Introduction

Long-period geomagnetic pulsations are common during substorms in the auroral zone, pulsations with periods greater than 150 s being called Pi3 type according to international classification. These irregular pulsations have been subdivided into two distinct groups namely PiP (Raspovov 1970) and Ps6 (Saito 1972). The groups are separated mainly by their occurrence in local time and by magnetic signature (Kiselev and Raspovov 1976). Ps6 pulsations are quasi-periodic with periods in the range 10–40 min and are strongest in the *Y* component of the magnetic field both on the ground and at high altitudes. They occur mainly in the morning hours and are closely correlated with auroral activity.

The magnetic variations reported here showed the characteristics of Ps6 pulsations, but were longer-lasting and stronger than those usually measured. They occurred over a local magnetic time period from 0430 to 0700. The peak to peak amplitudes in the *Y* and *Z* components were up to about 700 nT. The maximum intensity was measured at a latitude between Kiruna and Tromsø which made this event particularly suitable for study due to the reasonably good coverage of groundbased measurements in that area. Furthermore electric field measurements were carried out from balloons during the same time interval as the magnetic pulsations and they showed a clear correlation. A map showing the location of the observing stations is shown in Fig. 1.

Due to the fact that groundbased magnetic measurements alone cannot distinguish between numerous possible two- or three-dimensional equivalent current systems in the ionosphere and mag-

netosphere (Fukushima 1976) it is necessary to support them with other measurements in order to get a more complete physical description. Here we have used electric field and cosmic noise absorption measurements to put constraints on the three-dimensional model for the current system.

The characteristics of the Ps6 pulsations have been studied in some detail by Saito (1974, 1978). He proposed a mechanism with field-aligned currents at the eastern and western ends of the substorm westward electrojet and attributed Ps6 to the meandering of the current system during the course of the substorm from the midnight region toward both east and west. Kawasaki and Rostoker (1979) have suggested a three-dimensional current model of narrow longitudinal extent in which antiparallel Birke-land current sheets are linked by equatorial flowing ionospheric current.

In this study the pulsation event of 8 July 1975, an unusually strong and long-lasting Ps6 event, has been studied in detail. The results are compared with earlier suggested mechanisms, and a model of the three-dimensional current flow which agrees with the data is presented.

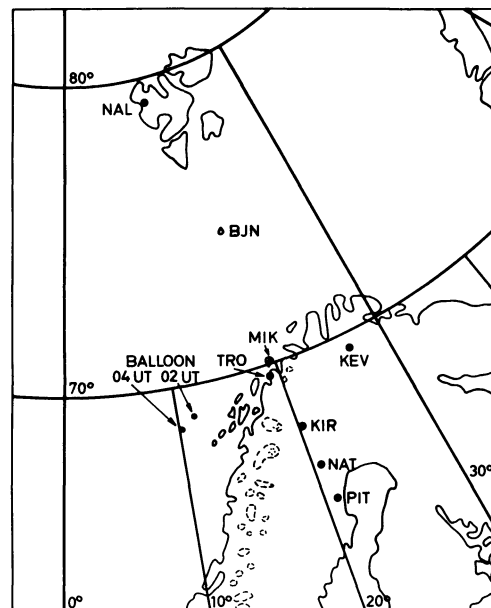


Fig. 1. Map showing the location of the observing stations and the balloon

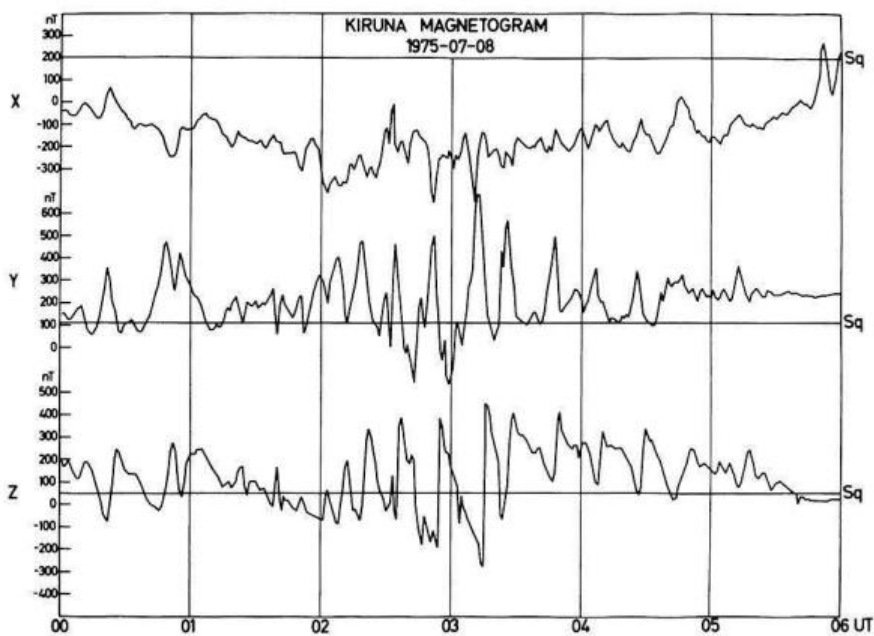


Fig. 2. Standard magnetogram, Kiruna

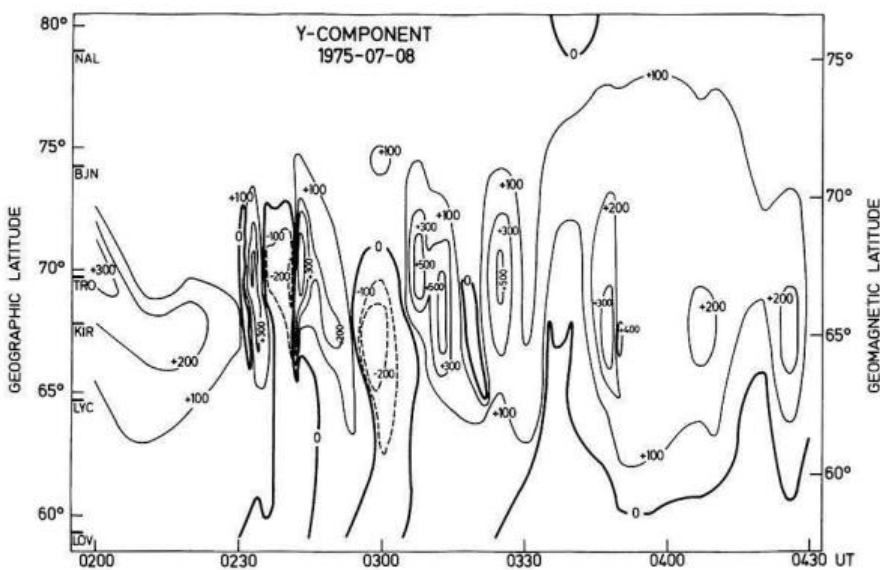


Fig. 3. Boström-Zaitsev diagram for the magnetic  $Y$  component

### Description of Measurements

The magnetic event observed by ground based magnetometers in Northern Scandinavia, 8 July 1975 between 0200 and 0500 UT, corresponding to 0430–0730 MLT, showed regular periodic variations. Figure 2 shows the magnetogram from Kiruna where large  $Z$  component variations (up to 700 nT) were recorded throughout the 3-h period. The positive excursions have time constants of less than one minute while those for the negative excursions are of the order of 20 min. The  $Y$  component showed symmetrical changes of up to 600 nT with peaks coinciding with the rapid positive excursions in the  $X$  component. The  $X$  component showed that the periodic structure was superimposed on a westward electrojet of about 500 nT.

Comparison with 3 years of magnetic recordings at Kiruna showed that the unique features of this event were the very long duration (most events were less than one hour) and the large amplitudes. Data from a chain of standard magnetic stations from

59° to 78° latitude (Fig. 1) have been used to locate the disturbance in latitude. The center varied very little during the night and was generally located between Kiruna and Tromsø, the latitudinal extent being about 5° as shown in Fig. 3 for the  $Y$  component in the form of a Zaitsev-Boström diagram (Zaitsev and Boström 1971).

The University of Münster operated a meridian chain of closely spaced magnetometers with high time resolution (10 s) at Mikkelvik (MIK, 70°04', 19°02'), Kiruna (KIR, 67°50', 20°25'), Nattavaara (NAT, 66°45', 21°00') and Piteå (PIT, 65°15', 21°35'). These stations constituted the first part of the Scandinavian Magnetometer Array which was built up during the years 1974–1976 (Küppers et al. 1979). The recordings from these stations are shown in Fig. 4. The  $A$  and  $B$  components are aligned along the  $x_{KI}$  and  $y_{KI}$  axes of the Kiruna system, respectively (cf. Küppers et al. 1979). Since those axes are perpendicular and parallel respectively to  $\Phi_i$  (KIR) = 64.8° with  $\Phi_i$  denoting the revised corrected geomagnetic latitude (Gustafsson 1970),  $A$  and  $B$  components may

7-8 JULY 1975

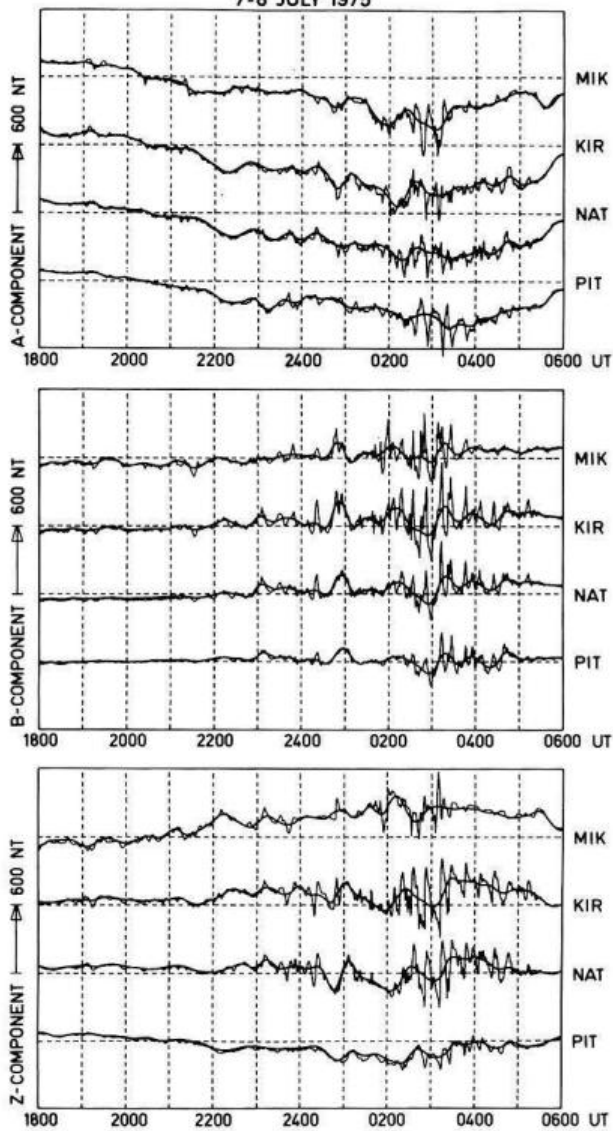


Fig. 4. Münster magnetograms, with low pass filtered ( $T > 30$  min) data superimposed

be regarded as corrected geomagnetic north and east components, respectively. In order to separate the 20-min variations from the more slowly varying contribution of the electrojet a filter (with the  $-6$  dB cutoff point at a period of 30 min) has been used; the low frequency signal, i.e., the slowly varying electrojet contribution has also been included in Fig. 4. The disturbance vectors discussed in this paper are measured relative to this new reference line and thus represent the more rapid variations.

In order to derive information about the particle precipitation during the present event, recordings from the riometers at Kiruna and Kevo ( $69^{\circ}45'$ ,  $27^{\circ}01'$ , Fig. 1) have been used. From Fig. 5 it can be seen that the recordings at both stations look very similar but that the absorption recorded at Kevo is delayed relative to Kiruna by 3–5 min. Kevo is located about 350 km east of Kiruna which means that this time delay corresponds to an eastward motion of the maximum absorption region with a velocity of a few km/s.

The 20-min variation is very pronounced in the riometer data

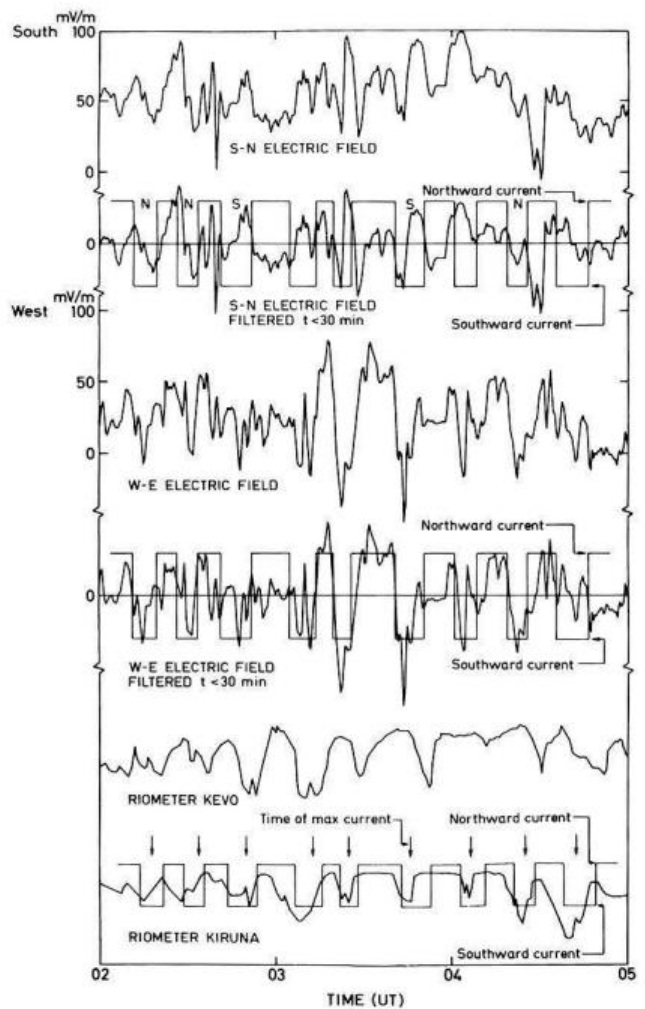
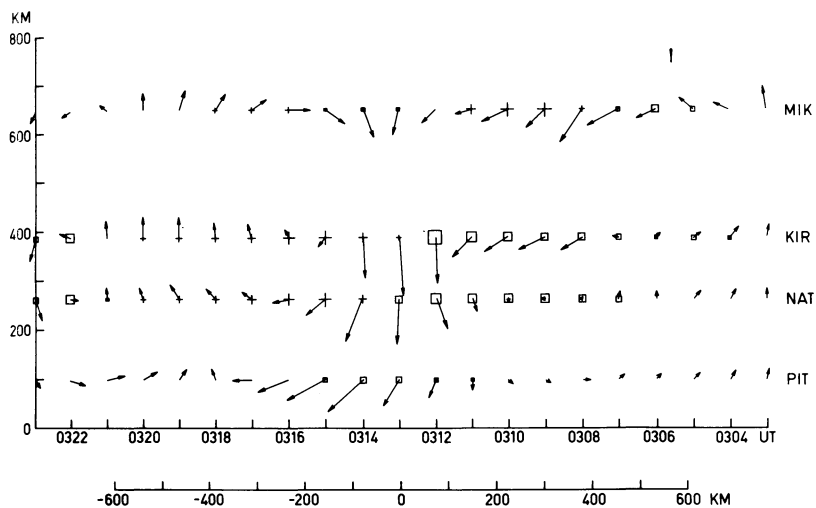


Fig. 5. Balloon electric field data and ground based riometer recordings. The periods of northward and southward magnetic equivalent current vectors, defined from the Münster magnetometers, have been drawn as a "square wave". The "square wave" has been shifted by 3 min when superimposed on the electric field recordings to compensate for the location of the balloon. The arrows indicate the time of due southward current

and shows good correlation with the magnetic variations of Figs. 2 and 4. Therefore, it may be concluded that the magnetic variations are closely related to precipitation of electrons of a few tens of keV.

The Danish Space Research Institute had a balloon equipped with electric field detectors a few hundred km west of Kiruna during the night discussed in this paper. The balloon was located as follows: at 0200 UT:  $68^{\circ}42'$ ,  $11^{\circ}21'$ ; at 0300 UT:  $68^{\circ}36'$ ,  $10^{\circ}46'$ ; at 0400 UT:  $68^{\circ}30'$ ,  $10^{\circ}00'$  (Fig. 1). The horizontal components of the electric field are shown in Fig. 5. These recordings show more structure than the absorption data but the 20-min variation can be identified easily particularly in the east-west component. Peak to peak amplitudes of more than 100 mV/m were recorded. It may also be seen from Fig. 5 that variations with periods greater than 30 min are very small in the east-west component and somewhat larger in the north-south component, although still smaller than the higher frequency components. It was mentioned earlier that a filter technique was used to separate the



**Fig. 6.** Two-cell equivalent current structure. The time has been drawn from right to left to illustrate a possible stable structure drifting in the eastward direction over the north-south magnetometer chain. A velocity of 1.3 km/s has been assumed. The signs + and □ refer to positive and negative Z components, respectively

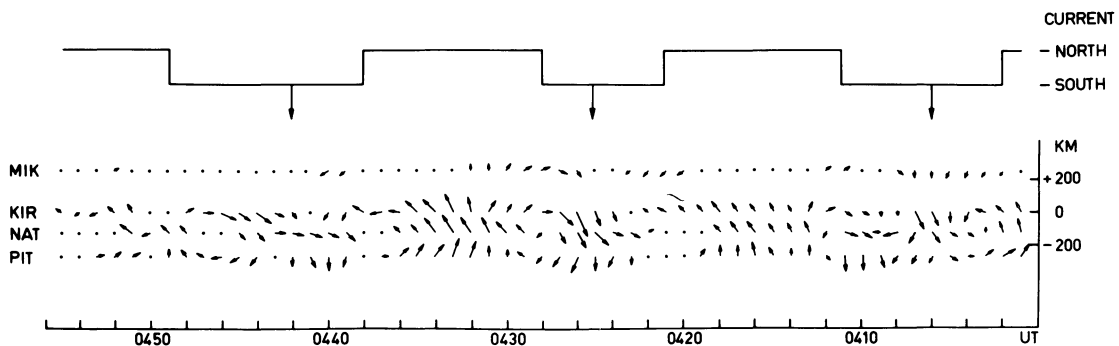
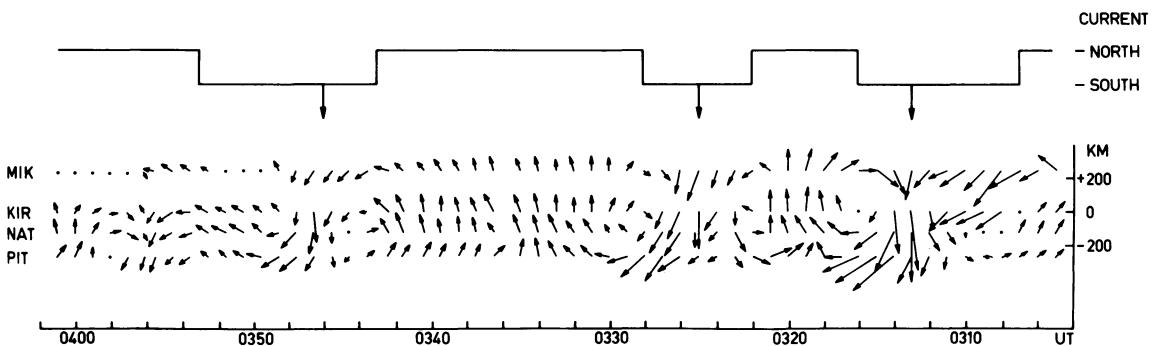
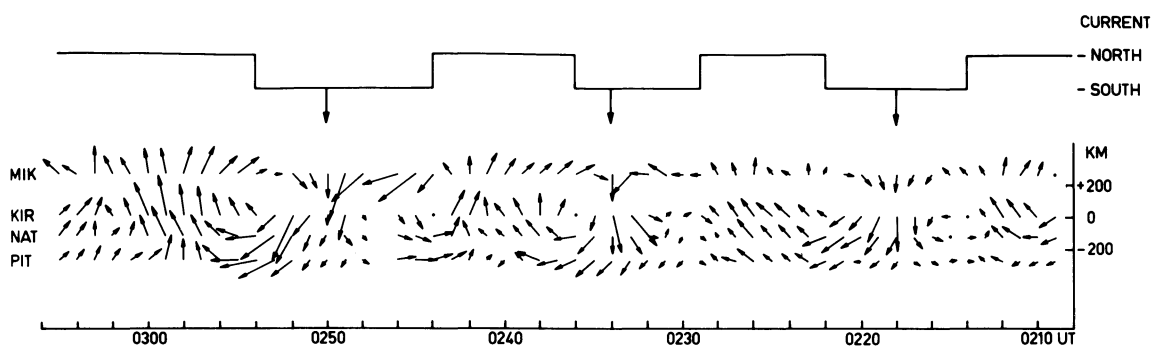


**Fig. 7.** Continuous current cell structures during the whole event similar to Fig. 6

current system due to the electrojet from the system that is attributable to variations with a period of about 20 min. Figure 4 shows that the northward  $A$  component was dominated by a rather steady electrojet during the interval of interest. On the other hand, the eastward  $B$  component was dominated by the 20-min variations. In the following a detailed description will be made of the magnetic data after it has been passed through the high pass filter.

In order to indicate the equivalent current pattern associated with the magnetic disturbance, the magnetic disturbance vectors at the four stations operated by the University of Münster have been rotated  $90^\circ$  clockwise. Figure 6 shows the equivalent current pattern for the time interval centered at 0313 UT, when a maximum in the eastward magnetic component corresponding to a southward current vector was observed. The time axis has been drawn from right to left to illustrate a possible stationary system moving in the eastward direction. The same horizontal and vertical distance scale is obtained in Fig. 6 if the assumption is made that the current pattern drifted with an eastward velocity of 1.3 km/s over the meridian-chain magnetic stations (as indicated by the riometer observations). The current pattern shows two cells with a southward current between them, where the largest current was also concentrated. Similar two cell patterns could be drawn for all maxima in the eastward magnetic component during the time interval 0200–0500 UT (see Fig. 7). The center of each current cell separates regions of current vectors with northward and southward components. The "square wave" in Fig. 6 corresponds to time intervals of a northward and southward component of the currents, and the arrows indicate the time of maximum southward current. The same square wave also been superimposed on the riometer recording from Kiruna in Fig. 5. A comparison between the magnetic and riometer data obtained at Kiruna as seen in Fig. 5 shows that the maximum in the absorption was closely correlated with the change from northward to southward directed equivalent currents but the time of maximum southward current was delayed relative to the maximum absorption. Therefore, maximum precipitation of electrons occurred inside the eastern counterclockwise current cell. At the balloon a similar time difference (2–3 min) between the maxima of the measured X-rays and eastward maxima of the electric field was observed (Iversen et al. 1977).

To illustrate the relation between the east-west electric field component and the equivalent current component the same square wave pattern was superimposed on the electric field measurements in Fig. 5, where the wave has been advanced 3 min relative to the balloon recording to compensate for the fact that the electric field measurements were made about 300 km west of Kiruna. The 3-min delay has been estimated from the measured difference between the riometer absorptions at Kiruna and Kevo, assuming the same velocity for the structures west of Kiruna. The observed time difference between the maximum eastward electric field at the balloon and southward current observed at Kiruna varied between 3 and 4 min. Although electric and magnetic measurements were not made at the same locations, there is good evidence that the eastward electric field corresponds to southward equivalent currents. The electric field measurements show considerable high frequency fluctuations and a rather steady bias but a good correspondence can be found between eastward and westward directed excursions of the electric field and southward and northward directed components of the equivalent currents, respectively.

The other component of the horizontal equivalent current (east-west direction) in the two cell pattern has the following be-

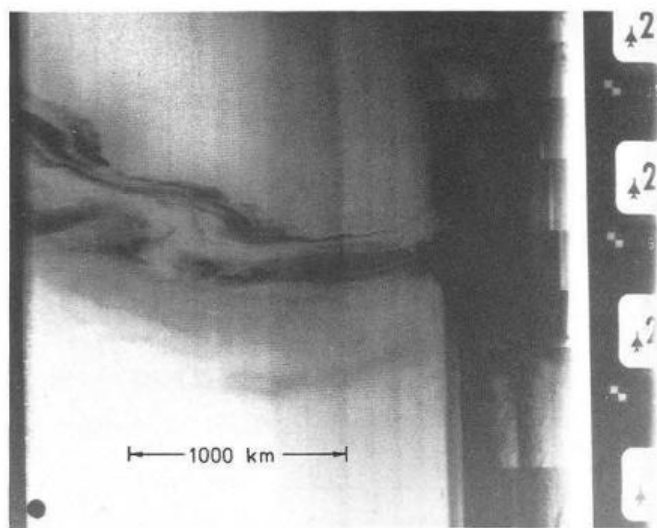


Fig. 8. DMSP picture of the aurora in the southern hemisphere at about 0140 UT

haviour: south of the latitudinal center line through the cells, the direction will change from eastward to westward at the time when the maximum southward current passes the meridian of the stations (see Fig. 6) and the opposite change occurs north of the center line. Therefore, the east-west component of the current vectors will show different temporal variations for recording stations north and south of the latitudinal center of the disturbance. The change from eastward to westward current has been indicated in Fig. 5 on the panel showing the north-south electric field component and marked  $N$  (also shifted by 3 min, see above). The change in the opposite sense has been marked  $S$ . It can be seen from Fig. 5 that the period of southward currents generally corresponds to large changes in the north-south component of the electric field. It may be noted that the electric field measurements of the north-south component showed short period variations, particularly in the time interval 0235–0245 UT, which can also be identified in the magnetic data north of Tromsø (see Fig. 3) but are not shown so clearly in Fig. 7. The lack of correspondence of the north-south electric field in a few cases is not unexpected and a time shift of a few minutes will give a good fit (the two measurements are made about 300 km apart and somewhat non-symmetrical patterns such as changes in drift velocity could cause that difference). The correspondence therefore suggests that the east-west current vectors and the north-south electric vectors are physically correlated.

The event discussed here occurred in the middle of the summer and no auroral data could be obtained in Scandinavia. However, the DMSP satellite recorded aurora in the southern hemisphere during the same time interval. Figure 8 shows the auroral image obtained at 0140 UT. Loop structures with a north-south extent of 200–300 km and a separation between the structures of about 900 km were recorded. Similar structures were observed on all the following satellite passes at 0322, 0403 and 0503 UT. The satellite pass at 0545 UT is shown in Fig. 9 where very clear loops can be seen. Comparing this with the magnetic observations in northern Scandinavia it may be concluded that auroral forms were observed in the southern hemisphere auroral zone which could correspond to the eastward travelling magnetic disturbances. A direct comparison cannot be made because the DMSP satellite traversed a region of the auroral oval whose fieldlines are con-

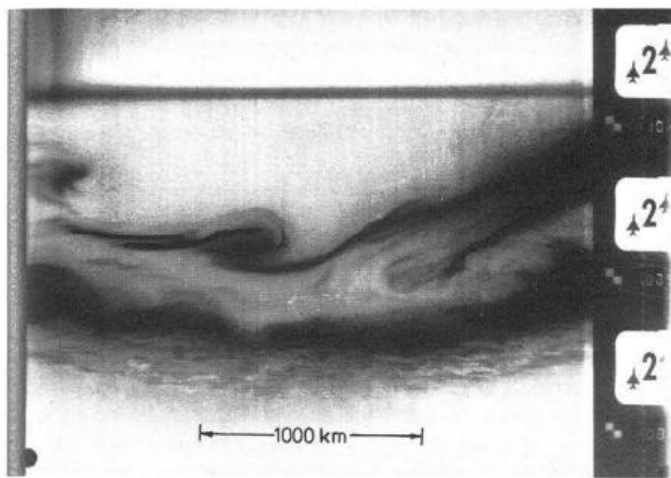


Fig. 9. DMSP picture of the aurora in the southern hemisphere at about 0545 UT

nected in the northern hemisphere to a region several thousand km west of Scandinavia.

Similar temporal variation to that observed by the groundbased and balloon measurements can also be seen in the ATS-6 magnetic field and energetic particle data (ATS-6 was at the time near the Kiruna longitude, personal communications McPherron and McIlwain, respectively). This shows that field aligned currents are observed at the equator along the same field lines. This will be the subject of a later study.

## Discussion

The event discussed in this report showed very regular variations in the magnetic field, particularly in the  $Y$  and  $Z$  components, for several hours. The magnetic variation, with the low frequency component ( $> 30$  min) removed has been displayed in Fig. 7 where nine consecutive events with very similar patterns in the equivalent current vectors can be noted. The apparent structure as seen by the magnetometers was a two-cell pattern east and west of a southward current and moving in the eastward direction at a velocity between 1 and 2 km/s, with the higher velocity at the beginning of the disturbance period. The intervals between the patterns were not of exactly equal lengths. The events occurred at 0218, 0234, 0250, 0313, 0325, 0346, 0406, 0425, and 0442 UT which means intervals of 16, 16, 23, 12, 21, 20, 19, and 17 min, respectively, between the events. Using an average velocity of 1.5 km/s this would give a spacing of 1000 to 2000 km between the two-cell structures.

The riometer absorption showed a one to one correlation with the magnetic events. The time when the absorption peak occurred could not be determined very accurately but in general the maximum in the absorption observed over Kiruna occurred close to the center of the eastern counterclockwise current cell and was not coincident with the southward current. This was also supported by the time difference between the electric field and X-ray measurements at the balloon.

The electric field as measured on a balloon a few hundred km west of Kiruna showed variations corresponding to the magnetic variations and the conclusion could be drawn that the orientations of the magnetic and electric field vectors in the east-west direction were coincident, to within the uncertainty of the measurements.

Let us now discuss the three-dimensional current system associated with the observed variations in magnetic and electric fields and riometer absorption. The observed magnetic field pattern could be explained by two possible equivalent current systems. One of these would be similar to a short north-south aligned Boström type 1 system (Boström 1964) and would consist of a pair of field-aligned line currents, about 100 km apart in the region of maximum southward equivalent current, (in Figs. 6 and 7) linked in the ionosphere by a southward directed Cowling current (Baumjohann et al. 1977). The other possible system would be somewhat similar to a Boström type 2 configuration. Here, we again have a pair of field-aligned currents, but now with the upward and downward directed ones located in the eastern and western cells, respectively. If the height-integrated Hall and Pedersen conductivities are homogeneous, the magnetic effects of field-aligned and Pedersen currents will cancel each other and ground-based magnetometers will observe only the clockwise and counterclockwise Hall current loops around the field-aligned currents (Fukushima 1976; Boström 1977).

The simultaneous observations of electric fields and riometer absorption give some evidence that this second equivalent current system comes closer to the real three-dimensional current system than the first one. Firstly, the maximum riometer absorption, which reflects energetic electron precipitation and hence upward field-aligned current flow (Klumpar et al. 1976; Kamide and Rostoker 1977; Klumpar 1979), tends to be located in the eastern cell and not in the region of maximum southward equivalent current. Secondly, the east-west electric field is parallel to the east-west magnetic field and perpendicular to the north-south equivalent current vectors. This indicated that the magnetic disturbances on the ground are caused solely by Hall-currents, as described in the second model.

In order to support the above discussion and to give some quantitative values, we have constructed a simplified numerical model for the dual equivalent current cell pattern centered on 0313 UT. Following Fukushima (1974) one can calculate the electric field in the ionosphere due to a field-aligned line-current pair by substituting for them a pair of positively and negatively charged fieldlines (the electric charge dissipating as a Pedersen current in the ionosphere from the footprints of those two fieldlines is assumed to be compensated by field-aligned current from the magnetosphere). The radial component of the electric field in the ionosphere is given by (with  $Q$  electric charge density per unit height from ionosphere to infinity):

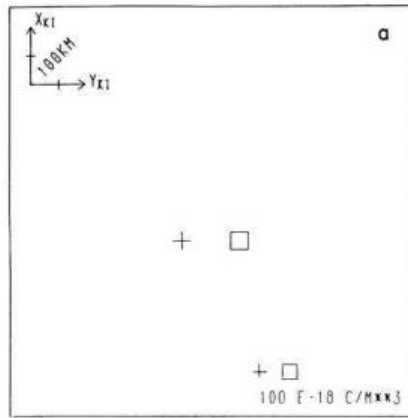
$$E_r(r, \lambda) = \pm Q/4\pi\epsilon r.$$

By assuming some distribution of height-integrated Hall and Pedersen conductivities, we can compute the ionospheric currents using the ionospheric Ohm's law. Subsequently the field-aligned currents may be determined from the divergence of the horizontal currents.

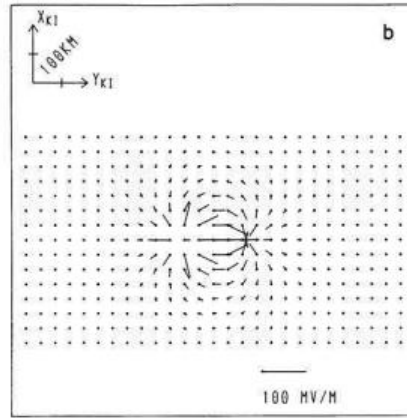
For numerical modelling we have divided the ionosphere into small cells each  $50 \times 50$  km and for each cell we have computed electric fields and currents in the manner described above. The height of the ionospheric current layer has been chosen as 100 km above the earth's surface in agreement with the average height of the westward electrojet after Kamide and Brekke (1977). The magnetic fields on the ground caused by the ionospheric-magnetospheric currents and by induced currents in a perfect conductor below 125 km depth (typical depth for periods of the order of 15 min, after Mareschal 1976), have been calculated using the Biot-Savart law.

The model parameters and the resultant equivalent current

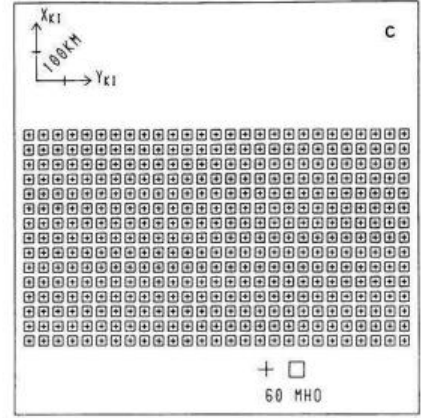
## COLUMN CHARGES



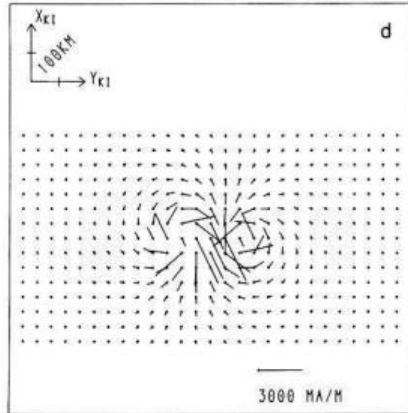
## IONOSPHERIC ELECTRIC FIELD



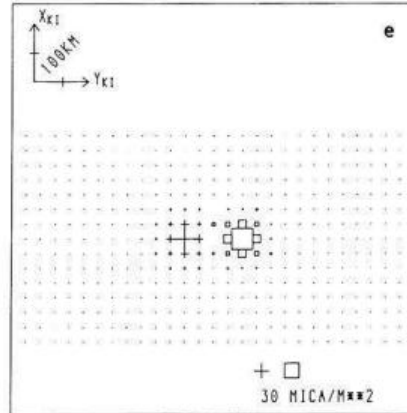
## IONOSPHERIC CONDUCTIVITY



## IONOSPHERIC CURRENTS



## FIELD-ALIGN CURRENTS



## EQ CURR GROUND

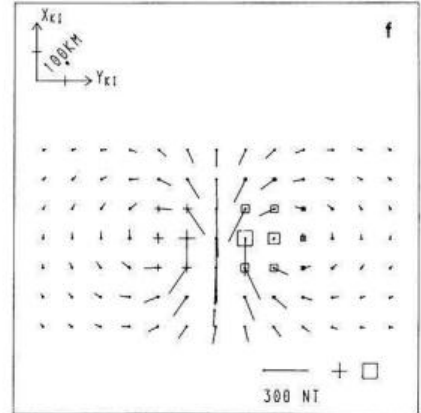


**Fig. 10a-f.** Parameters of the model current system and resultant equivalent current system on the ground. **a** Location of negatively (*square*) and positively (*cross*) charged fieldlines. **b** Ionospheric electric field vectors attributable to these charges. **c** Ionospheric Hall (*square*) and Pedersen (*cross*) conductivity. **d** Ionospheric currents. **e** Upward (*square*) and downward (*cross*) field aligned currents. **f** Equivalent currents on the ground; *squares* and *crosses* denote negative and positive *Z* components, respectively

vectors on the ground are displayed in Fig. 10. By assuming a positive and a negative line charge density of  $3 \cdot 10^{-7} \text{ Cm}^{-1}$  and a longitudinal spacing of 200 km (Fig. 10a) we obtained maximum westward electric fields of  $70 \text{ mVm}^{-1}$  and maximum eastward directed ones of  $40 \text{ mVm}^{-1}$  (Fig. 10b).

This would be equivalent to peak-to-peak amplitudes of  $110 \text{ mVm}^{-1}$  and hence in reasonable agreement with the observed values. Furthermore, we have assumed homogeneous Hall and Pedersen conductivities of 40 and  $20 \Omega^{-1}$ , respectively, which are in the range of those values given by Horwitz et al. (1978a, b). The assumption of uniform conductivity is probably too simple but good enough for our coarse model. The resultant ionospheric and field-aligned current densities are displayed in Fig. 10d-e and one may note maximum southward height-integrated Hall currents of the order of  $2 \text{ Am}^{-1}$  and a total up- and downward field-aligned current flow of about  $3 \cdot 10^5 \text{ A}$ . The Hall current density of  $2 \text{ Am}^{-1}$  is very high in comparison to about  $500 \text{ mA m}^{-1}$  found for the westward electrojet in the morning sector by Sulzbacher et al. (1980) and Baumjohann and Kamide (in press 1981). In addition, the field-aligned current in each of the double cells constitutes 10%–20% of the total field-aligned current flow in the midnight to forenoon sector (Iijima and Potemra 1976, 1978). The equivalent current vectors on the ground, caused by the three-dimensional current system (and the induced currents) are shown in Fig. 10f and we feel that the distribution comes rather close to that ob-

served around 0313 and displayed in Fig. 6. A comparison of horizontal and vertical components of Figs. 6 and 10f, also indicates that a depth of 125 km for the perfect conductor is a good estimate. Otherwise both horizontal and vertical components for the same model could not fit the observed data, since induced currents enhance the horizontal and reduce the vertical components of the external magnetic field. Lastly, we note that our model has been constructed only for one pair of field-aligned currents while the observations show a series of several pairs. However, the pairs are separated by more than 1000 km and since  $E$  varies as  $1/r$ , neighbouring pairs would affect each other's electric field only very slightly and would not change the overall pattern as displayed in Fig. 10.

Several previous studies have been carried out on eastward-travelling features along the morning auroral oval which could be related to the results presented here. Akasofu (1974) and Snyder and Akasofu (1974) reported on eastward drifting  $\Omega$ -bands. Tsunoda and Fremouw (1976) presented radar auroral signatures with eastward motions in the morning sector. Wescott et al. (1976) found anomalous behaviour of barium streaks in the vicinity of  $\Omega$ -bands indicating downward acceleration of electrons.

Baumjohann (1979) has shown a case where Ps6 pulsations are actually associated with eastward drifting  $\Omega$ -bands. He found eastward velocities of  $0.8 \text{ km s}^{-1}$  and also the equivalent double cell current pattern, consistent with the present results.

Saito (1974) and Saito and Yumoto (1978) investigated several models for Ps6 magnetic perturbations and concluded that the meandering current model proposed by Saito could explain most of the features in the Ps6 data. The model presented in this paper with pairs of east-west oriented, eastward-travelling Hall current loops, when superimposed on a westward electrojet, will produce a current system which is equivalent to the model proposed by Saito. But our model gives the real current configuration while Saito's model is an equivalent one based on magnetic data alone.

Kawasaki and Rostoker (1979) reported eastward-travelling regions of large magnetic perturbations with propagation velocities in the range 0.8–2 km/s, which seem comparable to those found in our event. They modelled the disturbances with a three-dimensional current system where antiparallel Birkeland current sheets were linked by an equatorward flowing ionospheric current. Although their three-dimensional model current system produces the same magnetic field perturbation pattern as our Hall current system, the riometer data, the electric field data and the magnetometer data do not, when taken together, support their model. As mentioned earlier the electron precipitation was located in the eastern cell and not in the region of the maximum equatorward equivalent current and it was also found that the east-west electric field was parallel to the appropriate magnetic field vectors.

*Acknowledgements.* We are greatly indebted to those past and present members of the magnetometer group at the University of Münster, who were involved in collecting the data. The magnetic observations were performed in cooperation with the Department of Plasma Physics of the Royal Institute of Technology and the Kiruna Geophysical Institute. The magnetometer chain observations and the work of W. Baumjohann were supported financially by grants from the Deutsche Forschungsgemeinschaft.

We would like to thank Mrs. H. Ranta, Geophysical Observatory, Sodankylä for the riometer data and Mr. S. Berger, Auroral Observatory, Tromsø for the magnetic data from Tromsø and Ny-Ålesund. The DMSP images were provided by the US Air Force Weather Service.

## References

- Akasofu, S-I. A study of auroral displays photographed from the DMSP-2 satellite and from the Alaska meridian chain of stations. *Space Sci. Rev.* **16**, 617–725, 1974
- Boström, R. A model of the auroral electrojets. *J. Geophys. Res.* **69**, 4983–5000, 1964
- Boström, R. Current systems in the ionosphere and magnetosphere. In: Radar probing of the auroral plasma. A. Brekke, ed. pp 257–284. Oslo: Universitetsforlaget 1977
- Baumjohann, W., Gustafsson, G., Küppers, F. Large-amplitude rapid magnetic variations during a substorm (abstract only). *EOS Trans. Am. Geophys. Union* **58**, 718, 1977
- Baumjohann, W. Spatially inhomogeneous current configurations as seen by the Scandinavian Magnetometer Array. In: Proceeding of the International Workshop on Selected Topics of Magnetospheric Physics, Japanese IMS Committee, ed. pp 35–40. Tokyo: 1979
- Baumjohann, W., Kamide, Y. Joint two-dimensional observations of ground magnetic and ionospheric electric fields associated with auroral zone currents – 2. Three-dimensional current flow in the morning sector during substorm recovery. *J. Geomagn. Geoelectr.*, in press 1981
- Irukushima, N. Equivalent current pattern for ground geomagnetic effect when the ionospheric conductivity is discontinuous at the foot of a field-aligned current sheet. *Rep. Ionos. Space Res. Jpn.* **28**, 147–151, 1974
- Irukushima, N. Generalized theorem for no ground magnetic effect of vertical currents connected with Pedersen currents in the uniform-conductivity ionosphere. *Rep. Ionos. Space Res. Jpn.* **30**, 35–40, 1976
- Gustafsson, G. A revised corrected geomagnetic coordinate system. *Ark. Geofys.* **5**, 595–617, 1970

- Horwitz, J.L., Doupnik, J.R., Banks, P.M. Chatanika radar observations of the latitudinal distributions of auroral zone electric fields, conductivities, and currents. *J. Geophys. Res.* **83**, 1463–1481, 1978a
- Horwitz, J.L., Doupnik, J.R., Banks, P.M., Kamide, Y., Akasofu, S-I. The latitudinal distributions of auroral zone electric fields and ground magnetic perturbations and their response to variations in the interplanetary magnetic field. *J. Geophys. Res.* **83**, 2071–2084, 1978b
- Iijima, T., Potemra, T.A. The amplitude distribution of field-aligned currents at northern high latitudes observed by Triad. *J. Geophys. Res.* **81**, 2165–2174, 1976
- Iijima, T., Potemra, T.A. Large-scale characteristics of field-aligned currents associated with substorms. *J. Geophys. Res.* **83**, 599–615, 1978
- Iversen, I.B., Madsen, M.M., Ullaland, S., Brønstad, K., Bjordal, J. Electric field and X-ray measurements with balloons during a magnetic storm. Presented at IAGA Assembly 1977
- Kamide, Y., Brekke, A. Altitude of the eastward and westward auroral electrojets. *J. Geophys. Res.* **82**, 2851–2853, 1977
- Kamide, Y., Rostoker, G. The spatial relationship of field-aligned currents and auroral electrojets to the distribution of nightside auroras. *J. Geophys. Res.* **82**, 5589–5608, 1977
- Kawasaki, K., Rostoker, G. Perturbation magnetic fields and current systems associated with eastward drifting auroral structures. *J. Geophys. Res.* **84**, 1464–1480, 1979
- Kiselev, B.V., Raspopov, O.M. Excitation of Pi3 type pulsations during substorm. In: Proceedings of IAGA meeting on unmanned observatories in Antarctica, T. Nagata, ed. pp 88–96. Tokyo: 1976
- Klumpar, D.M. Relationship between auroral particle distributions and magnetic field perturbations associated with field-aligned currents. *J. Geophys. Res.* **84**, 6524–6532, 1979
- Klumpar, D.M., Burrows, J.R., Wilson, M.D. Simultaneous observations of field-aligned currents and particle fluxes in the post-midnight sector. *Geophys. Res. Lett.* **3**, 395–398, 1976
- Küppers, F., Untiedt, J., Baumjohann, W., Lange, K., Jones, A.G. A two-dimensional magnetometer array for ground-based observations of auroral zone electric currents during the International Magnetospheric Study (IMS). *J. Geophys.* **46**, 423–450, 1979
- Mareschal, M. On the problem of simulating the earth's induction effects in modelling polar magnetic substorms. *Rev. Geophys. Space Phys.* **14**, 403–409, 1976
- Raspopov, O.M. Sur la diagnostique des changes electriques dans la magnetosphere de la terre. *Ann. Geophys.* **26**, 751–759, 1970
- Saito, T. Some topics for the study of the mechanism of magnetospheric substorm by means of rocket observation in the auroral zone. *Antarctic Record* **43**, 65–69, 1972
- Saito, T. Examination of the models for the substorm-associated magnetic pulsation Ps6. *Sci. Rep. Tohoku Univ. Ser. 5 Geophys.* **22**, 35–59, 1974
- Saito, T. Long-period irregular magnetic pulsation, Pi3. *Space Sci. Rev.* **21**, 427–467, 1978
- Saito, T., Yumoto, K. Comparison of the two-snake model with the observed polarization of the substorm associated magnetic pulsation Ps6. *J. Geomagn. Geoelectr.* **30**, 39–45, 1978
- Snyder, A.L., Akasofu, S-I. Major auroral substorm features in the dark sector observed by a USAF DMSP satellite. *Planet. Space Sci.* **22**, 1511–1517, 1974
- Sulzbacher, H., Baumjohann, W., Potemra, T.A. Coordinated magnetic observations of morning sector auroral zone currents with Triad and the Scandinavian Magnetometer Array: a case study. *J. Geophys.* **48**, 7–17, 1980
- Tsunoda, R.T., Fremouw, E.J. Radar auroral substorm signatures. 2. East-west motions. *J. Geophys. Res.* **81**, 6159–6168, 1976
- Wescott, E.M., Stenbaek-Nielsen, H.C., Hallinan, T.J., Davis, T.N., Peek, H.M. The Skylab Barium plasma injection experiments. 2. Evidence for a double layer. *J. Geophys. Res.* **81**, 4495–4502, 1976
- Zaitsev, A.N., Boström, R. On methods of graphical displaying of polar magnetic disturbances. *Planet. Space Sci.* **19**, 643–649, 1971

Received June 27, 1980; Revised Version October 20, 1980

Accepted October 20, 1980